Polynuclear Mn^{II} Complexes with Chloroacetate Bridge − Syntheses, Structure, and Magnetic Properties

Gema Fernández,[a] Montserrat Corbella,*[a] José Mahía,[b] and Miguel A. Maestro[b]

Keywords: Manganese / Crystal structures / Magnetic properties / EPR spectroscopy / Bridging ligands

Three new polynuclear Mn^{II} complexes with chloroacetate bridges were obtained and characterized by X-ray diffraction: $[Mn_3(\mu\text{-}ClCH_2COO)_6(bpy)_2]$ (**1**), $[Mn_2(\mu\text{-}ClCH_2COO)_2(phen)_4](ClO_4)_2$ (**2**), and $[Mn(\mu\text{-}ClCH_2COO)_2(phen)]_n$ (**3**). The Mn···Mn distance for **1** (3.624 Å) is smaller than for **2** (4.613 Å) and **3** (4.530 Å); this is in agreement with the number of carboxylate bridges. The three compounds show a weak antiferromagnetic coupling. The J values are –3.82 cm^{-1} for **1**, –0.85 cm^{-1} for **3**, and no coupling was observed for **2**. Each compound showed a characteristic EPR spectrum at 4 K. Simulation of these spectra could be obtained with D = –0.16 cm^{-1} and E = –0.015 cm^{-1} for compound **1**, and D = –0.045 cm^{-1} and E = –0.004 cm^{-1} for compound **2**.

Introduction

Manganese is found in several metalloproteins. Usually, the manganese ion binds the protein through the carboxylate groups of aspartate or glutamate. In coordination chemistry, this sort of ligand is often found bridging two metal ions, which helps polymerization. This fact is also observed in biological systems, where the reaction centers have between 1 and 4 Mn ions.

The Mn^{II} ion usually plays a structural and/or hydrolytic role; however, it is also found in the reduced form in manganese redox enzymes. There are some dinuclear Mn−carboxylate active sites, e.g. catalase,[1] aminopeptidase,[2] arginase.[3] Recently, it has been shown that one pyrophosphatase needs 3 Mn^{II} ions for catalytic activity.[4] Further, interest in Mn^{II}−carboxylate chemistry has arisen due to the fact that the spectroscopic properties of Mn^{II} have been used as a probe for the sites that normally bind other metal ions. Understanding the structural and magnetic properties of different Mn^{II}−carboxylate complexes will therefore be useful in gaining insight into the structural details of the active site(s) that may influence the chemical mechanisms of catalysis.

Some dinuclear complexes with carboxylate bridges are reported in the literature, with $[Mn_2(\mu\text{-}H_2O)(\mu\text{-}RCOO)_2]^{2+}$,[5−7] $[Mn_2(\mu\text{-}OH)(\mu\text{-}RCOO)_2]^{+}$,[8,9] and $[Mn_2(\mu\text{-}OR)(\mu\text{-}RCOO)_2]^{+}$ cores.[10−14] There are also some dinuclear compounds which only have carboxylate bridges, e.g. three,[9,15−18] two,[19−29] or one.[30,31]

On the other hand, the number of trinuclear Mn^{II} complexes with bridging carboxylate groups is limited.[32−37] Finally, the number of one-dimensional Mn^{II} polymers is increasing,[28,29,39−44] but very few have two carboxylate bridges.[19,45−47]

In this paper we report the isolation and characterization of three new Mn^{II} compounds, with the same carboxylate ligand, $ClCH_2COO^-$. The nuclearity of these compounds differs; $[Mn_3(\mu\text{-}ClCH_2COO)_6(bpy)_2]$ (**1**) is trinuclear, $[Mn_2(\mu\text{-}ClCH_2COO)_2(phen)_4](ClO_4)_2$ (**2**) is dinuclear, and $[Mn(\mu\text{-}ClCH_2COO)_2(phen)]_n$ (**3**) is a one-dimensional compound. The structural characterization of these compounds was achieved by X-ray diffraction, and both their magnetic behavior and their EPR spectra were studied.

Results and Discussion

Syntheses

In a previous paper we studied the reactivity of $Mn(RCOO)_2{\cdot}nH_2O$ (R = 2-ClC_6H_4, 3-ClC_6H_4, and 4-ClC_6H_4) with 2,2′-bipyridine.[19] Mn^{II}/bpy ratios of 1:$^2/_3$ and 1:1 were considered, but each carboxylate had a preferred nuclearity (trinuclear complex or chain). In the present work we studied the analogous reaction of $Mn(ClCH_2COO)_2{\cdot}2H_2O$ with various bidentate amines, 2,2′-bipyridine, and 1,10-phenanthroline. Independent of the Mn^{II}/amine ratio, two different compounds were found for the same carboxylate. The 2,2′-bipyridine ligand gave a trinuclear complex $[Mn_3(\mu\text{-}ClCH_2COO)_6(bpy)_2]$ (**1**), while the 1,10-phenanthroline ligand gave a chain $[Mn(\mu\text{-}ClCH_2COO)_2(phen)]_n$ (**3**).

[a] Departament de Química Inorgànica, Universitat de Barcelona, Martí i Franquès 1−11, 08028 Barcelona, Spain
E-mail: montse.corbella@qi.ub.es
[b] Servicios Xerais de Apoio á Investigación, Universidade da Coruña, Edificio Anexo Facultade de Ciencias
15071 A Coruña, Spain

In the synthesis of the dinuclear compound $[Mn_2(\mu\text{-}ClCH_2COO)_2(phen)_4](ClO_4)_2$ (**2**), a 1:2:1 ratio of Mn^{II}/phen/ClO_4^- was considered. Attempts to obtain the analogous compound with bpy led to the formation of the more stable mononuclear compound $[Mn(bpy)_3](ClO_4)_2$.

Crystal Structures

$[Mn_3(\mu\text{-}ClCH_2COO)_6(bpy)_2]$ (1)

The structure of compound **1** is depicted in Figure 1; selected bond lengths and angles are collected in Table 1; **1** consists of a linear array of three Mn^{II} ions with an Mn(2)−Mn(1)−Mn(2_2) angle of 179.98°. Each Mn(2)···Mn(1) pair is separated by 3.624 Å, a similar distance to that reported for the analogous complex with acetate bridges $[Mn_3(\mu\text{-}CH_3COO)_6(bpy)_2]$ (3.614 Å).[32] For the complex with benzoate ligands $[Mn_3(\mu\text{-}PhCOO)_6(bpy)_2]$,[34] this distance is a bit shorter (3.588 Å). Mn(1) is located on a crystallographic inversion center, and it is bridged to both Mn(2) by three chloroacetate ligands. Two of these ligands coordinate through the two oxygen atoms ($\mu_{1,3}$-$ClCH_2COO$), while the third carboxylate group coordinates through just one oxygen atom ($\mu_{1,1}$-$ClCH_2COO$). In this case, the other oxygen atom chelates through a weak bond the terminal Mn(2) ion. This unusual coordination mode of the carboxylate group provokes a great distortion around Mn(2). The two $\mu_{1,3}$-carboxylate groups are similar, with greater $Mn(1)-O_{carb}$ distances (av. 2.174 Å) than $Mn(2)-O_{carb}$ distances (av. 2.095 Å). The same is observed for the $\mu_{1,1}$-carboxylate, the $Mn(1)-O_{bridge}$ distance is 2.217 Å, while the $Mn(2)-O_{bridge}$ distance is 2.151 Å. For the acetate complex,[32] these distances are very similar (2.201 and 2.155 Å), however, for the benzoate complex,[34] the $Mn_{central}-O_{bridge}$ distance is 2.239 Å, while the $Mn_{terminal}-O_{bridge}$ distance is 2.286 Å. A similar difference is found for the Mn(2)−O(5)−Mn(1) angle. This angle is 112.12° for complex **1**, 112.2° for the acetate complex, and 104.94° for the benzoate complex. Another important difference between complexes with aliphatic and aromatic carboxylate groups is the $Mn_{terminal}-O_{terminal}$ distance. For the $\mu_{1,1}$-carboxylate, this distance is 2.611 Å with $ClCH_2COO^-$, 2.605 Å with CH_3COO^-; however, this distance is shorter with $PhCOO^-$ (2.274 Å) and quite similar to the $Mn_{terminal}-O_{bridge}$ distance. Therefore, the carboxylate is important for the localization or delocalization of the π-system−COO^-. The benzoate favors delocalization, while the aliphatic carboxylate, with or without a chloro substituent, favors the asymmetry of the $-COO^-$ group.

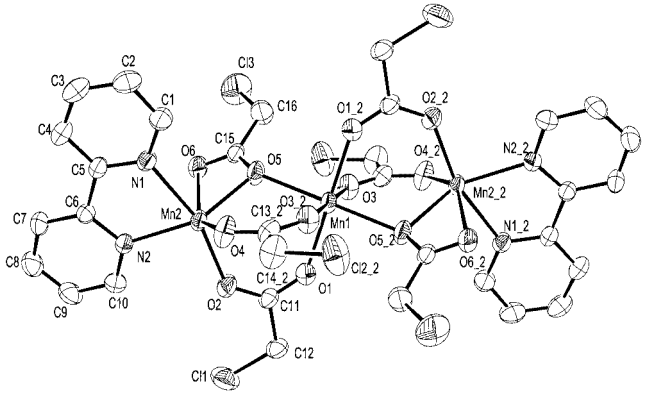

Figure 1. ORTEP drawing of complex **1**

The six-coordination of Mn(2) is completed by a 2,2′-bipyridine ligand. The acute angles O(5)−Mn(2)−O(6) (53.81°) and N(1)−Mn(2)−N(2) (73.19°) and the difference between the bond lengths Mn(2)−N and Mn(2)−O lead to

Table 1. Selected bond lengths [Å] and angles [°] with estimated standard deviations (e.s.d.s) in parentheses for $[Mn_3(\mu\text{-}ClCH_2COO)_6(bpy)_2]$ (**1**)

Mn(1)−O(1)	2.155(3)	Mn(2)−O(2)	2.090(3)
Mn(1)−O(1_2)	2.155(3)	Mn(2)−O(4)	2.099(3)
Mn(1)−O(3_2)	2.194(2)	Mn(2)−O(5)	2.151(2)
Mn(1)−O(3)	2.194(2)	Mn(2)−O(6)	2.611(3)
Mn(1)−O(5)	2.217(2)	Mn(2)−N(2)	2.219(3)
Mn(1)−O(5_2)	2.217(2)	Mn(2)−N(1)	2.246(3)
Mn(1)···Mn(2)	3.624(1)	Mn(1)−O(5)−Mn(2)	112.13(11)
O(1)−Mn(1)−O(1_2)	180.00(14)	O(2)−Mn(2)−O(4)	93.95(13)
O(1)−Mn(1)−O(3_2)	89.48(11)	O(2)−Mn(2)−O(5)	98.50(11)
O(1_2)−Mn(1)−O(3_2)	90.52(11)	O(4)−Mn(2)−O(5)	97.34(11)
O(1)−Mn(1)−O(3)	90.52(11)	O(2)−Mn(2)−N(2)	90.66(11)
O(1_2)−Mn(1)−O(3)	89.48(11)	O(4)−Mn(2)−N(2)	120.38(11)
O(3_2)−Mn(1)−O(3)	180.0(2)	O(5)−Mn(2)−N(2)	140.51(10)
O(1)−Mn(1)−O(5)	91.35(10)	O(2)−Mn(2)−N(1)	163.14(11)
O(1_2)−Mn(1)−O(5)	88.65(10)	O(4)−Mn(2)−N(1)	90.23(11)
O(3_2)−Mn(1)−O(5)	89.12(9)	O(5)−Mn(2)−N(1)	97.16(11)
O(3)−Mn(1)−O(5)	90.88(9)	N(2)−Mn(2)−N(1)	73.19(10)
O(1)−Mn(1)−O(5_2)	88.65(10)	O(2)−Mn(2)−O(6)	103.08(11)
O(1_2)−Mn(1)−O(5_2)	91.35(10)	O(4)−Mn(2)−O(6)	148.00(11)
O(3_2)−Mn(1)−O(5_2)	90.88(9)	O(5)−Mn(2)−O(6)	53.81(8)
O(3)−Mn(1)−O(5_2)	89.12(9)	N(1)−Mn(2)−O(6)	81.28(10)
O(5)−Mn(1)−O(5_2)	180.0(2)	N(2)−Mn(2)−O(6)	86.70(9)

a distorted octahedral geometry around the terminal Mn ions. On the other hand, the central Mn atom linked to six oxygen atoms has a more regular octahedral environment (Mn−O distances from 2.155 to 2.217 Å and O−Mn−O angles from 88.65 to 91.35°).

$[Mn_2(\mu\text{-}ClCH_2COO)_2(phen)_4](ClO_4)_2\cdot 2CH_2Cl_2$ (2)

The structure of the cationic complex of compound **2** is depicted in Figure 2. Selected bond lengths and angles are listed in Table 2. The molecule contains a crystallographic inversion center, relating both halves of the dinuclear unit. There are two perchlorate anions, and two molecules of solvent (CH_2Cl_2) captured in the crystal lattice for each dinuclear unit.

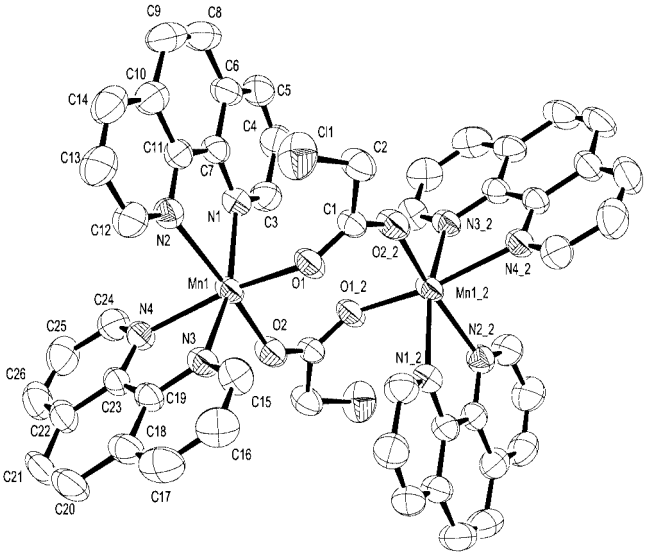

Figure 2. ORTEP drawing of the cation $[Mn_2(\mu\text{-}ClCH_2COO)_2(phen)_4]^{2+}$ in complex **2** showing the *syn-anti* conformation of the carboxylate bridges

Table 2. Selected bond lengths [Å] and angles [°] with estimated standard deviations (e.s.d.s) in parentheses for $[Mn_2(\mu\text{-}ClCH_2COO)_2(phen)_4](ClO_4)_2\cdot 2CH_2Cl_2$ (**2**)

Mn(1)−O(1)[a]	2.129(3)	Mn(1)−N(4)	2.271(4)
Mn(1)−O(2)	2.150(3)	Mn(1)−N(2)	2.327(4)
Mn(1)−N(1)	2.275(4)	Mn(1)−N(3)	2.278(4)
Mn(1)···Mn(1_2)	4.613(2)	O(1)−Mn(1)−O(2)	99.92(13)
O(1)−Mn(1)−N(4)	161.83(13)	N(4)−Mn(1)−N(3)	73.61(13)
O(2)−Mn(1)−N(4)	84.62(12)	N(1)−Mn(1)−N(3)	161.15(14)
O(1)−Mn(1)−N(1)	90.48(12)	O(1)−Mn(1)−N(2)	90.03(13)
O(2)−Mn(1)−N(1)	100.25(13)	O(2)−Mn(1)−N(2)	167.79(13)
N(4)−Mn(1)−N(1)	106.13(13)	N(4)−Mn(1)−N(2)	88.10(13)
O(1)−Mn(1)−N(3)	88.28(12)	N(1)−Mn(1)−N(2)	72.40(13)
O(2)−Mn(1)−N(3)	98.49(13)	N(3)−Mn(1)−N(2)	88.79(13)

[a] Symmetry codes: a: $-x + 2, -y + 1, -z + 1$.

The manganese ions are bridged by two chloroacetate ligands, in a *syn-anti* fashion. Six-coordination on each manganese ion is completed by two chelating 1,10-phenanthroline groups. The interatomic Mn···Mn distance of 4.613 Å is a bit longer than Mn···Mn distances found in analogous complexes with only two bridging *syn-anti* carboxylates; $[Mn_2(\mu\text{-}CH_3COO)_2(bpy)_4](ClO_4)_2$ (4.583 Å),[20] $[Mn_2(\mu\text{-}PhCOO)_2(bpy)_4](ClO_4)_2$ (4.509 Å).[19] When a third bridging ligand is present, e.g. another carboxylate,[9,16−18] aqua,[5−7] hydroxo,[8,9] or phenoxo[10−13] group, the Mn···Mn distance becomes smaller (4.03−3.35 Å).

The Mn−O distances are 2.129 Å ($Mn-O_{anti}$) and 2.151 Å ($Mn-O_{syn}$), which are shorter than the Mn−N distances (2.271−2.327 Å). Moreover, the N(1)−Mn(1)−N(2) angle (72.4°) and N(3)−Mn(1)−N(4) angle (73.6°) are far from 90°, due to the restricted geometry of the phenanthroline ligands. Both factors contribute to the distortion of the octahedral geometry around the manganese ions.

For this compound, $d(Mn-O_{anti}) < d(Mn-O_{syn})$, while for the acetate[20] and the benzoate[19] complexes $d(Mn-O_{anti}) > d(Mn-O_{syn})$.

$[Mn(\mu\text{-}ClCH_2COO)_2(phen)]_n$ (3)

The structure consists of an infinite zigzag chain, as shown in Figure 3. Selected bond lengths and angles are presented in Table 3. The manganese atoms in the chain are bridged by two chloroacetate ligands coordinated in a *syn-anti* fashion. The six-coordination of each metal center is completed by one phenanthroline ligand. Surprisingly, the interatomic Mn···Mn distance (4.530 Å) is shorter than the distance found for complex **2** (4.613 Å). Both compounds have the same bridging ligands, and the same terminal amine. The Mn···Mn distance for $[Mn(\mu\text{-}3\text{-}ClC_6H_4COO)_2(bpy)]_n$,[19] where the carboxylate bridge is also coordinated in a *syn-anti* fashion, is 4.515 Å. However, for $[Mn_2(\mu\text{-phth})(phen)_4]_n(ClO_4)_{2n}$ (phth= isophthalate),[47] where both manganese ions are bridged by two carboxylate groups coordinated in a *syn-syn* mode, the Mn···Mn distance is longer (4.86 and 4.66 Å).

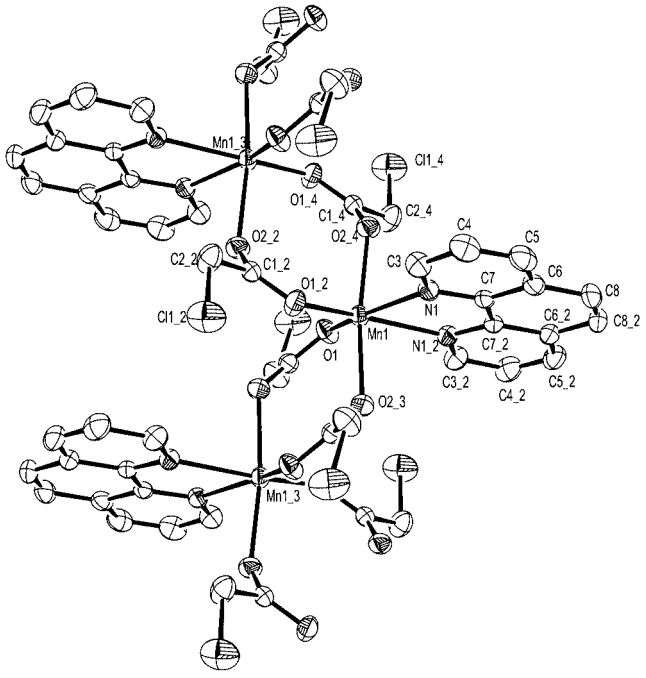

Figure 3. Plot of the one-dimensional complex **3**

Table 3. Selected bond lengths [Å] and angles [°] with estimated standard deviations (e.s.d.s) in parentheses for $[Mn(\mu\text{-}ClCH_2COO)_2(phen)]_n$ (**3**)

Mn(1)−O(1)[a]	2.1341(14)	Mn(1)−O(1_2)	2.1341(14)
Mn(1)−O(2_3)	2.1829(18)	Mn(1)−O(2_4)	2.1829(18)
Mn(1)−N(1)	2.3057(17)	Mn(1)−N(1_2)	2.3057(17)
Mn(1)···Mn(1_3)	4.530(2)	O(1)−Mn(1)−N(1)	156.96(6)
O(1)−Mn(1)−O(1_2)	114.51(9)	O(1_2)−Mn(1)−N(1_2)	156.96(6)
O(1)−Mn(1)−O(2_3)	97.95(6)	O(2_3)−Mn(1)−O(2_4)	172.73(7)
O(1)−Mn(1)−O(2_4)	86.00(6)	O(1_2)−Mn(1)−O(2_4)	97.95(6)
O(1)−Mn(1)−N(1_2)	87.46(6)	O(1_2)−Mn(1)−O(2_3)	86.00(6)
O(2_3)−Mn(1)−N(1)	90.11(6)	O(1_2)−Mn(1)−N(1)	87.46(6)
O(2_3)−Mn(1)−N(1_2)	84.00(5)	O(2_4)−Mn(1)−N(1)	84.00(5)
N(1)−Mn(1)−N(1_2)	71.88(8)	O(2_4)−Mn(1)−N(1_2)	90.11(6)

[a] Symmetry codes: a: $-x + 2, y, -z + 3/2$; b: $-x + 2, -y, -z + 1$; c: $x, -y, z + 1/2$.

There are two equivalent Mn−N distances (2.306 Å), and the Mn−O distance is slightly shorter for the carboxylate oxygen atom *trans* to the phenanthroline nitrogen atom [$d(Mn-O_{transN}) = 2.134$ Å] than for the two carboxylate oxygen atoms *trans* to each other [$d(Mn-O_{transO}) = 2.183$ Å]. The O_{transN} are O_{syn}, while the O_{transO} atoms are O_{anti}, therefore $d(Mn-O_{anti}) > d(Mn-O_{syn})$. This is observed for the analogous chain $[Mn(\mu\text{-}3\text{-}ClC_6H_4COO)_2(bpy)]_n$,[19] but differs from the behavior shown by compound **2**. Moreover, the Mn−O distances are longer for the one-dimensional compound **3** than for the dinuclear complex **2**. The N−Mn−N angle (71.88°) is similar to the values found for the same amine group in compound **2**. Thus, the geometry around each manganese atom is distorted octahedral.

The chain runs parallel to the *c* axis, of the *C*2/*c* space group, in a helix-type conformation, and the phenanthroline ligands are stacked, with a phen···phen distance of 7.491 Å. The smallest interchain metal separation is 9.598 Å.

Magnetic Properties

Magnetic susceptibility data were recorded for the three complexes, from room temperature to 4 K. The $\chi_M T$ vs. T plots for compounds **1**−**3** are shown in Figure 4. For the dinuclear complex **2**, the $\chi_M T$ value is ca. 8.8 $cm^3mol^{-1}K$ in the range room temperature to 18 K. This value is very close to that expected for two uncoupled Mn^{II} ions. The decrease in $\chi_M T$ below this temperature may be a result of the antiferromagnetic interactions (intra- or intermolecular), or of the ZFS (Zero Field Splitting), which is usually small for Mn^{II} ions.

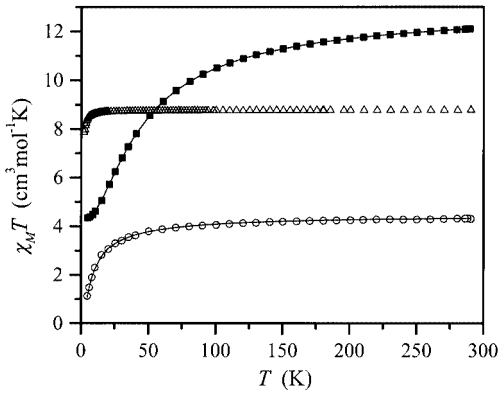

Figure 4. $\chi_M T$ vs. T plot for $[Mn_3(\mu\text{-}ClCH_2COO)_6(bpy)_2]$ (**1**) (■), $[Mn_2(\mu\text{-}ClCH_2COO)_2(phen)_4](ClO_4)_2$ (**2**) (Δ), and $[Mn(\mu\text{-}ClCH_2COO)_2(phen)]_n$ (**3**) (O); the solid line is the best fit to the experimental data

For the trinuclear complex **1**, $\chi_M T$ decreases from 12.10 $cm^3mol^{-1}K$ at 290 K to 4.34 $cm^3mol^{-1}K$ at 4.8 K. The $\chi_M T$ value at room temperature, is smaller than the expected value for three uncoupled Mn^{II} ions (13.125 $cm^3mol^{-1}K$). This is indicative of an antiferromagnetic coupling, as confirmed by the decrease in $\chi_M T$ when T decreases. At low temperature, the $\chi_M T$ value is indicative of an $S = 5/2$ spin state.

Taking into account the structure of this compound, the spin Hamiltonian considered would be $\boldsymbol{H}_S = -J(\boldsymbol{S}_1\cdot\boldsymbol{S}_2+\boldsymbol{S}_2\cdot\boldsymbol{S}_1) - J'(\boldsymbol{S}_2\cdot\boldsymbol{S}_2)$. However, the magnetic interaction between the terminal manganese ions ($Mn_2\cdots Mn_2$) in a linear complex is negligible ($J' \approx 0$),[19,32] and only the $Mn_1\cdots Mn_2$ interaction (J) is considered. The best fit corresponds to $J = -3.82$ cm^{-1}, $g = 2.01$ and $R = 1.9\ 10^{-7}$.

For the one-dimensional compound **3**, $\chi_M T$ values decrease monotonically from 4.18 $cm^3mol^{-1}K$ at 298 K to 1.10 $cm^3mol^{-1}K$ at 5 K. The magnetic susceptibility data were analyzed by the analytical expression derived by Fisher[48] for an infinite chain of classical spins based on the Hamiltonian $\boldsymbol{H} = -J\Sigma\boldsymbol{S}_i\cdot\boldsymbol{S}_{i+1}$, for local spin values of $S = 5/2$. The best fit corresponds to $J = -0.89$ cm^{-1}, $g = 2.01$ and $R = 2.6\ 10^{-4}$.

The three compounds reported here have the same bridging ligands, through which the magnetic interaction arises. In spite of this fact, a certain difference in the coupling constant could be appreciated. The trinuclear complex **1** presents a major Mn···Mn interaction. It differs from the other two compounds in the coordination mode of the bridge; there are two $ClCH_2COO$ ligands coordinated in a *syn-syn* fashion, and a third carboxylate ligand, $\mu_{1,1}$-$ClCH_2COO$, which provides a new interaction pathway, through only one oxygen atom. Unfortunately, the number of compounds described in the literature with this kind of structure it is limited,[32−36] and to the best of our knowledge, a magnetic study was reported for only three of them.[32,33,35] The compound $[Mn_3(\mu\text{-}AcO)_6(BiC_6H_4$-

Table 4. Comparison of the structural parameters (distances [Å] and angles [°]) and magnetic interaction (J [cm^{-1}]) for the Mn^{II} polynuclear complexes

3 carboxylate bridges	$d(Mn_t-O_b)$[a]	$d(Mn_c-O_b)$[a]	$d(Mn_t-O_t)$[a]	α[a]		J[b]	Ref.
$[Mn_3(\mu\text{-}ClCH_2COO)_6(bpy)_2]$ (**1**)	2.151	2.217	2.611			−3.81	*
$[Mn_3(\mu\text{-}AcO)_6(bpy)_2]$	2.155	2.201	2.605	112.2		−4.40	[32]
$[Mn_3(\mu\text{-}AcO)_6(pybim)_2]$[c]	2.132	2.235	2.823	109.1		−3.80	[35]
$[Mn_3(\mu\text{-}AcO)_6(BiPhMe)_2]$[d]	2.17−2.27	2.18−2.24	2.31−2.79	112.3		−4.8	[33]
2 carboxylate bridges	d_{anti}[e]	d_{syn}[e]	α[e]	β[e]	γ[e]	J	Ref.
$[Mn_2(\mu\text{-}ClCH_2COO)_2(phen)_4]^{2+}$ (**2**)	2.129	2.150	99.92	138.2	135.31	ca. 0	*
$[Mn_2(\mu\text{-}PhCOO)_2(bpy)_4]^{2+}$	2.139	2.118	103.55	151.9	126.38	−1.76	[19]
$[Mn_2(\mu\text{-}AcO)_2(tpa)_2]^{2+}$ [f]	2.160	2.060	107.6	133.5	128.0	−1.94	[22]
$[Mn(\mu\text{-}ClCH_2COO)_2(phen)]_n$ (**3**)	2.183	2.134	97.95	123.9	130.91	−0.89	*
$[Mn(\mu\text{-}3\text{-}ClC_6H_4COO)_2(bpy)]_n$	2.196	2.104	100.50	134.4	131.92	−1.72	[19]

[a] Mn_t = Mn terminal; O_b = O_1 of the $\mu_{1,1}$-carboxylate; Mn_c = Mn central; O_t = the other O of the $\mu_{1,1}$-carboxylate; α = $Mn_tO_bMn_c$ angle. [b] With the same Hamiltonian and J_{13} = 0; *: this work. [c] pybim = *N*-[2-(2-pyridylmethyleneamino)phenyl]pyridine-2-carboxamide. [d] BiPhMe = 2-[methoxy(1-methyl-1*H*-imidazol-2-yl)phenylmethyl]-1-methyl-1*H*-imidazole. [e] d_{anti} = $d(Mn-O_{anti})$; d_{syn} = $d(Mn-O_{syn})$; α = $O_{anti}MnO_{syn}$ angle; β = $MnO_{syn}C$ angle; γ = $MnO_{anti}C$ angle. [f] tpa = tris(2-pyridylmethyl)amine.

$Me)_2]$[33] presents different isomeric forms with different Mn−O distances; in general $d(Mn_t-O_b) \approx d(Mn_c-O_b)$. For **1**, $[Mn_3(\mu\text{-}AcO)_6(pybim)_2]$[35] and $[Mn_3(\mu\text{-}AcO)_6(bpy)_2]$[32] (Table 4), $d(Mn_t-O_b) < d(Mn_c-O_b)$ and is markedly different from $d(Mn_t-O_t)$. The magnetic interaction for all of these compounds is of the same order. Normally, a carboxylate group that is coordinated in a *syn-syn* fashion gives a moderate antiferromagnetic coupling.

Compounds **2** and **3** have the same kind of bridge, two $ClCH_2COO$ groups coordinated in a *syn-anti* fashion; however, while the one-dimensional compound shows a certain antiferromagnetic interaction, in the dinuclear complex this interaction is practically zero. The magnetic interaction through a *syn-anti* carboxylate bridge should be very sensitive to small structural changes. Figure 5 shows a schematic representation of the relative orientations of two magnetic orbitals for these compounds. The Mn···Mn interaction could be affected by several factors: the Mn−O distance, the $O_{anti}-Mn-O_{syn}$ angle (α), the $Mn-O_{syn}-C$ angle (β), the $Mn-O_{anti}-C$ angle (γ) and also by the non-planarity of the bridge (τ). Small changes in these parameters could change the overlap through the carboxylate group. Table 4 shows some structural parameters for these compounds in comparison with analogous compounds described in the literature. For the one-dimensional compound **3**, a major difference between d_{anti} and d_{syn} can be observed, probably due to the fact that *trans* to O_{anti} there is another O_{anti} of the chain. The same trend could be observed in the analogous compound with $3\text{-}ClC_6H_4COO$,[19] but the angle around O_{syn} is large, and a greater antiferromagnetic interaction was found.

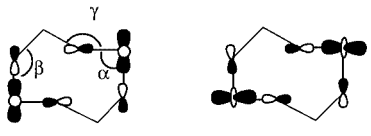

Figure 5. Relative orientation of two manganese(II) magnetic orbitals and their interaction through the carboxylate bridges with a *syn-anti* conformation in the $[Mn_2(\mu\text{-}ClCH_2COO)_2]^{2+}$ core (dinuclear compound **2** and one-dimensional compound **3**)

Compounds **2** and **3** have similar α angles, but they show some differences in the β and γ angles. The dinuclear compound presents a set of larger angles (α, β, γ) than the chain, in spite of the fact that the O−C−O angles are similar. For the dinuclear complex **2**, where d_{syn} is similar to d_{anti}, the angles around O_{syn} (β) and O_{anti} (γ) are also similar, while for $[Mn_2(\mu\text{-}PhCOO)_2(bpy)_4]^{2+}$ [19] β > γ, and for $[Mn_2(\mu\text{-}AcO)_2(tpa)_2]^{2+}$ [22] β is only slightly greater than γ, and d_{anti} and d_{syn} are markedly different. Both compounds show an antiferromagnetic interaction, in contrast to that found in compound **2** where no magnetic coupling is observed. The major asymmetry could contribute to a major overlap through the bridge.

EPR Spectra

The three compounds studied here show weak Mn···Mn interactions, so even at low temperatures several spin states may be populated. This may lead to many possible transitions, and thus to a complicated EPR spectrum.[30] At room temperature all the complexes show a broad signal centered at $g \approx 2$. However, at 4 K, the spectrum of each compound is quite different (Figure 6, solid line).

The spectrum at room temperature for the trinuclear complex (compound **1**) presents a broad signal (ΔH_{pp} = 1055 G) centered at $g \approx 2$. The intensity of this signal decreases with temperature. At 60 K, the shape of the spectrum is the same as the shape of the spectrum at room temperature. Variable-temperature EPR spectra are shown in Figure 7. At 17 K, the spectrum shows a new intense and broad band at $g \approx 3.3$, and another less intense feature at $g \approx 8$, which is already present at 40 K. At 4 K, the spectrum becomes complicated; the signal at $g \approx 2$ almost disappears, while many signals at high field and the more intense signals at low field ($g \approx 6.7$ and $g \approx 4$) remain. This spectrum is similar to that reported for the acetate[32] and chlorobenzoate[19] analogues. Considering the J value of

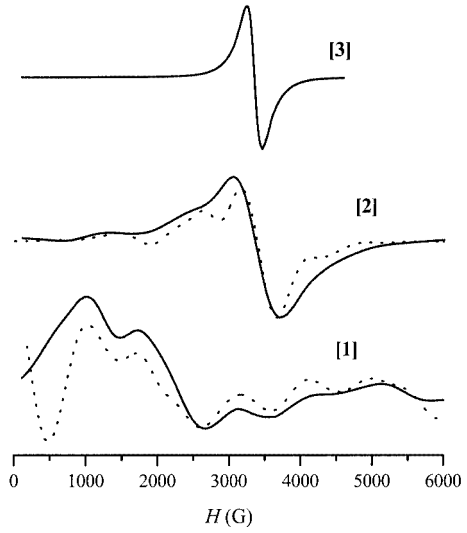

Figure 6. Comparative X-band EPR spectra of a microcrystalline sample at 4 K of complexes $[Mn(\mu\text{-}ClCH_2COO)_2(phen)]_n$ (**3**), $[Mn_2(\mu\text{-}ClCH_2COO)_2(phen)_4](ClO_4)_2$ (**2**), and $[Mn_3(\mu\text{-}ClCH_2COO)_6(bpy)_2]$ (**1**) (solid line); simulated spectra of complexes **2** and **1** (dashed line)

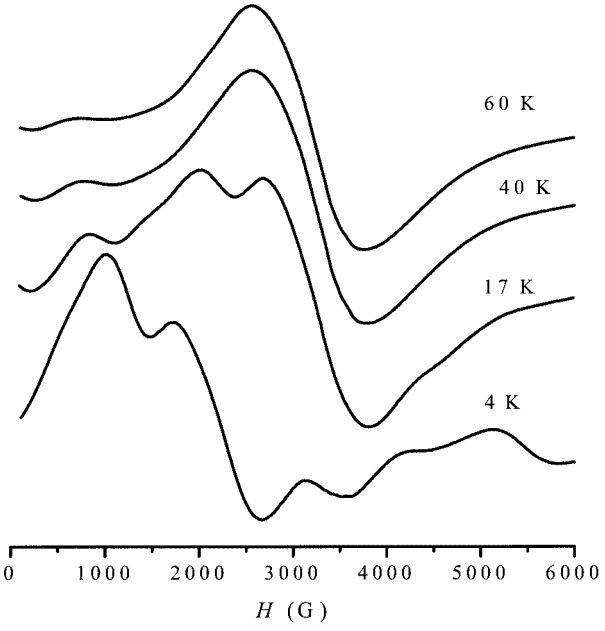

Figure 7. Variable-temperature X-band EPR spectra of $[Mn_3(\mu\text{-}ClCH_2COO)_6(bpy)_2]$ (**1**)

-3.82 cm^{-1}, at 4 K only the ground state ($S_T = 5/2$) may be populated. For the simulation of the experimental spectrum only the ground state was considered, and therefore, the possible transitions between the ground state and the excited states were not considered for the simulation. In spite of this approach, a quite good simulation has been obtained with $D = -0.16$ cm^{-1}, $E = -0.015$ cm^{-1}, $g_x = 2.20$, $g_y = 1.98$, $g_z = 1.95$ and a bandwidth of 270 G. (Figure 6, dashed line).

The EPR spectra at different temperatures for the dinuclear complex (compound **2**) show a broad signal centered at $g \approx 2$. Variable-temperature EPR spectra are shown in

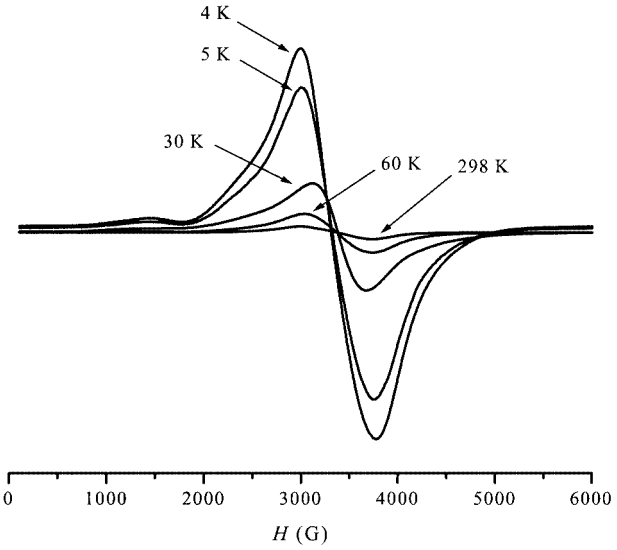

Figure 8. Variable-temperature X-band EPR spectra of $[Mn_2(\mu\text{-}ClCH_2COO)_2(phen)_4](ClO_4)_2$ (**2**)

Figure 8. The intensity of the signal increases when the temperature decreases. At 4 K, the broad signal centered at $g \approx 2$, with a $\Delta H_{pp} = 650$ G, is flanked by one feature at $g \approx 2.8$ and another at $g \approx 5.2$. Considering the fact that the Mn···Mn interaction is negligible, the spectrum can be considered to be that of an isolated Mn^{2+} ion. A good simulation could be obtained with $D = -0.045$ cm^{-1}, $E = -0.004$ cm^{-1}, and an isotropic $g = 2.06$ (Figure 6, dashed line). For the simulation of the spectrum, a bandwidth of 200 G was considered. With a bandwidth of 300 G a superimposable spectrum could be obtained. The variation in the intensity of the spectrum with temperature is due to the ZFS. For both simulations (for compounds **1** and **2**), a spin state of $S = 5/2$ was considered. For compound **2**, with no coupling between the Mn^{2+} ions, the ZFS parameters correspond to each Mn center of the dinuclear complex. The distortion around the metal ion is small, and the D and E values are also small. For compound **1**, the spin state of $S = 5/2$ is as a result of the Mn···Mn interaction in the trinuclear complex. This system shows a central Mn^{2+} ion, with a regular octahedral geometry, and two terminal Mn^{2+} ions with a greatly distorted geometry. The ZFS parameters include the single-ion ZFS for each manganese center, and the ZFS arising from spin-coupling. In this case, the values for D and E are greater than for the dinuclear complex where the distortion is smaller.

The spectrum of the chain (complex **3**) presents a single band centered at $g \approx 2$ at room temperature, with a peak-to-peak line width of 147 G. The broadness of the band increases at 4 K ($\Delta H_{pp} = 220$ G), and no change in position is observed (Figure 6). This behavior was also observed for the similar compound $[Mn(\mu\text{-}3\text{-}ClC_6H_4COO)_2(bpy)]_n$.[19]

Conclusion

With the same carboxylate bridging (chloroacetate) it was possible to obtain complexes of different nuclearity; dinuc-

lear, trinuclear and one-dimensional compounds. There are two factors that influence these results: the bidentate blocking ligand (phenanthroline or bipyridine), and the presence of perchlorate anions in the solution. The trinuclear complex was only obtained with the less rigid ligand, bipyridine, and surprisingly, it was not possible to obtain the ionic dinuclear complex with this amine. With the phenanthroline ligand, a neutral one-dimensional compound and the ionic dinuclear compound were obtained. The trinuclear complex **1** shows two *syn-syn* $ClCH_2COO$ bridges and one $\mu_{1,1}$-$ClCH_2COO$ bridge; this kind of bridge was also found in the arginase.[3] The observed Mn···Mn distance for **1** (3.624 Å) is slightly greater than for the arginase (3.3 Å), and very close to the Mn···Mn distance of the manganese-substituted ribonucleotide reductase (ca. 3.6 Å).[49] On the other hand, the dinuclear complex **2** and the one-dimensional compound **3** show greater values for the Mn···Mn distances (ca. 4.6 Å).

The magnetic measurement showed an antiferromagnetic Mn···Mn interaction. This antiferromagnetism is very small due to the presence of only carboxylate bridges, and the *J* value depends on the number and the coordination mode of the carboxylate bridges: $|J|_{trinuclear} > |J|_{chain} > |J|_{dinuclear}$. For compound **2**, with $J \approx 0$, the set of *d*(Mn−O), α, β, γ, and τ can probably give a small overlap through the bridge, then $J_{AF} \approx J_F$.

It is possible to differentiate the trinuclear complex **1** from the other two complexes **2** and **3** from their EPR spectrum at 4 K. The simulation of the EPR spectrum at this temperature for both compounds **1** and **2** give a *E*/*D* ratio of ca. 0.09. However, for the trinuclear complex **1**, the ZFS parameters *D* and *E* are bigger than for the dinuclear complex **2**.

Experimental Section

Syntheses: All manipulations were performed under aerobic conditions. Reagent grade solvents were used without further purification and organic reagents were used as received. $Mn(ClCH_2COO)_2{\cdot}2H_2O$ was synthesized by the reaction of $MnCO_3$ and $ClCH_2COOH$ in hot water. After several hours, the solution was filtered and the solvent was removed by evaporation giving a pale pink precipitate of the desired product. Yield ca. 70%. $C_4H_8Cl_2MnO_6$ (277.95): calcd. C 17.28, H 2.90; found C 17.5, H 2.9. ***Caution:*** Perchlorate salts of metal complexes with organic ligands are potentially explosive. Only a small amount of material should be prepared, and it should be handled with caution.

$[Mn_3(\mu\text{-}ClCH_2COO)_6(bpy)_2]$ (1): This compound was synthesized by adding an ethanolic solution of 2,2′-bipyridine (0.18 g, 1.2 mmol) to a solution of $Mn(ClCH_2COO)_2{\cdot}2H_2O$ (0.50 g, 1.8 mmol) in EtOH (30 mL) and H_2O (1 mL). The resulting mixture was left undisturbed at room temperature for several days. Yellow crystals suitable for X-ray determination were formed. Yield 0.36 g (ca. 58%). $C_{32}H_{28}Cl_6Mn_3N_4O_{12}$ (1038.11): calcd. C 37.02, H 2.72, N 5.40; found C 37.5, H 2.8, N 5.5. IR (cm^{-1}): $\tilde{\nu}$ = 1631 (vs), 1446 (m), 1407 (s), 1249 (m), 1242 (m), 795 (m), 769 (m).

$[Mn_2(\mu\text{-}ClCH_2COO)_2(phen)_4](ClO_4)_2$ (2): $Mn(ClCH_2COO)_2{\cdot}2H_2O$ (0.42 g, 1.5 mmol) and sodium perchlorate monohydrate (0.21 g, 1.5 mmol) were mixed in $EtOH/CH_2Cl_2$ (1:1, 50 mL). 1,10-Phenanthroline (0.54 g, 3.0 mmol), dissolved in the same solvent mixture, was then added to the solution, which immediately turned yellow. The solution was left undisturbed in a refrigerator for several days. Yellow crystals, stable only at low temperatures, were formed. Yield 0.73 g (ca. 80%). $C_{52}H_{36}Cl_4Mn_2N_8O_{12}$ (1216.58): calcd. C 51.34, H 2.98, N 9.21; found C 50.6, H 3.1, N 9.0 . IR (cm^{-1}): $\tilde{\nu}$ = 1650 (vs), 1624 (vs), 1520 (s), 1430 (vs), 1150 (vs), 1130 (vs), 1095 (vs), 854 (vs), 736 (vs), 643 (s).

$[Mn(\mu\text{-}ClCH_2COO)_2(phen)]_n$ (3): This compound was synthesized by mixing ethanolic solutions (total volume: 60 mL) of $Mn(ClCH_2COO)_2{\cdot}2H_2O$ (0.50 g, 1.8 mmol) and 1,10-phenanthroline (0.32 g, 1.8 mmol). The pale yellow precipitate formed was filtered and washed in ether. Recrystallization from $EtOH/H_2O$ (9:1) yielded pale yellow crystals suitable for X-ray determination. Yield 0.64 g (ca. 84%). $C_{16}H_{12}Cl_2MnN_2O_4$ (422.12): calcd. C 45.53, H 2.87, Cl 16.80, N 6.64; found C 44.9, H 2.8, Cl 16.5, N 6.5. IR (cm^{-1}): $\tilde{\nu}$ = 1657 (vs), 1614 (vs), 1524 (m), 1413 (s), 1250 (m), 848 (m), 775 (m), 735 (m), 700 (m).

Spectral and Magnetic Measurements: Infrared spectra (4000−400 cm^{-1}) were recorded from KBr pellets with a Perkin−Elmer 380-B spectrophotometer. Magnetic susceptibility measurements were carried out using a Faraday-type magnetometer (MANICS DSM8) equipped with an Oxford CF 1200 S helium continuous-flow cryostat working in the temperature range 4−300 K. Diamagnetic corrections were estimated from Pascal Tables. The agreement factor considered to fit the experimental data to the corresponding equation is defined as $R = \Sigma(Y_i^{exp} - Y_i^{cal})^2/\Sigma(Y_i^{exp})^2$. The best fit corresponds to the minimum value of *R*. EPR spectra were recorded at X-band (9.4 GHz) frequencies using a Bruker ESP-300E spectrometer, from room temperature to 4 K.

EPR Simulation: A program written by H. Weihe[50] was used to simulate powder EPR spectra. The simulation was performed by generating the energy matrix for each orientation of the molecule relative to the magnetic field. The resonance condition for each transition was then found by successive diagonalizations and iterations of the energy matrix, and the relative intensities were calculated from the eigenvectors multiplied by the appropriate Boltzmann factor at 4 K. Summation of all the transitions over the whole space, where each transition is represented by a differentiated Gaussian curve, gives the simulated spectrum. The spin Hamiltonian used for the simulation include the ZFS parameters *D* and *E*.

Crystallographic Data Collection and Refinement: Suitable single crystals of $[Mn_3(\mu\text{-}ClCH_2COO)_6(bpy)_2]$ (**1**, needle, yellow, dimensions 0.50 × 0.10 × 0.10 mm), $[Mn_2(\mu\text{-}ClCH_2COO)_2(phen)_4](ClO_4)_2{\cdot}2CH_2Cl_2$ (**2**, prism, yellow, dimensions 0.50 × 0.30 × 0.25 mm) and $[Mn(\mu\text{-}ClCH_2COO)_2(phen)]_n$ (**3**, prism, yellow, dimensions 0.50 × 0.30 × 0.20 mm) were used for the structure determination. X-ray data were collected using a Bruker SMART CCD area detector single-crystal diffractometer, with graphite-monochromatized Mo-K_α radiation (λ = 0.71073 Å), using the -ω scan method. A total of 1271 frames of intensity data were collected for each compound. The first 50 frames were recollected at the end of data collection to monitor for decay. The integration process yielded a total of 6812 reflections for **1**, 8061 for **2**, and 4543 for **3**, of which 4855 [*R*(int) = 0.0287], 5123 [*R*(int) = 0.0195], and 2059 [*R*(int) = 0.0191], respectively, were independent. Absorption corrections were applied using the SADABS[51] program (maximum and minimum transmission coefficients, 0.875 and 0.548 for **1**; 0.814 and 0.674 for **2**; and 0.765 and 0.602 for **3**). The structures were solved using the Bruker SHELXTL-PC[52] software by direct

Table 5. Crystallographic details for compounds **1**, **2**·2CH_2Cl_2, and **3**

	1	**2**	**3**
Empirical formula	$C_{32}H_{28}Cl_6Mn_3N_4O_{12}$	$C_{54}H_{40}Cl_8Mn_2N_8O_{12}$	$C_{16}H_{12}Cl_2MnN_2O_4$
M	1038.10	1386.42	422.12
Space group	$P\bar{1}$	$P\bar{1}$	$C2/c$
cryst system	triclinic	triclinic	monoclinic
Z	1	1	4
a [Å]	8.247(1)	11.506(3)	19.702(5)
b [Å]	10.298(1)	12.198(4)	11.386(5)
c [Å]	13.560(1)	12.215(2)	7.491(5)
α [°]	69.170(2)	87.660(2)	90
β [°]	79.242(1)	63.963(1)	93.892(5)
γ [°]	72.340(2)	74.40(2)	90
V [Å^3]	1021.6(1)	1477.8(7)	1676.6(1)
ρ(calcd.) [g/cm^3]	1.687	1.558	1.672
$\mu_{calcd.}$ [mm^{-1}]	1.369	0.856	1.130
Radiation (Mo-K_α) [Å]	0.70173	0.70173	0.70173
T [K]	298(2)	298(2)	298(2)
θ range for data collection	1.6−28.3	1.7−25.0	2.1−28.2
Final R indices[a]	$R1 = 0.0593$	$R1 = 0.0650$	$R1 = 0.0375$
[$I > 2\sigma(I)$]	$wR2 = 0.1506$	$wR2 = 0.1951$	$wR2 = 0.0996$
Final R indices	$R1 = 0.0845$	$R1 = 0.0803$	$R1 = 0.0420$
[for all data]	$wR2 = 0.1689$	$wR2 = 0.2125$	$wR2 = 0.1027$

[a] $R1 = \Sigma||F_o| - |F_c||/\Sigma|F_o|$ and $wR2 = \{\Sigma[w(F_o^2 - F_c^2)^2]/\Sigma[w(F_o^2)^2]\}^{1/2}$.

methods and refined by full-matrix least-squares methods on F^2. Hydrogen atoms were included in calculated positions and refined in the riding mode. The Cl(2) atom in compound **1** was refined in two different positions with partial occupation factors of 0.63 and 0.37. For **1**, convergence was reached at a final $R1 = 0.0593$ [for $I > 2\sigma(I)$], $wR2 = 0.1689$ [for all data], 269 parameters, with allowance for the thermal anisotropy for all non-hydrogen atoms. The weighting scheme employed was $w = [\sigma^2(F_o^2) + (0.1032 \cdot P)^2]$, $P = (|F_o|^2 + 2|F_c|^2)/3$; and the goodness of fit on F^2 was 1.001 for all observed reflections. For **2**, convergence was reached at a final $R1 = 0.0650$ [for $I > 2\sigma(I)$], $wR2 = 0.2125$ [for all data], 379 parameters, with allowance for the thermal anisotropy for all non-hydrogen atoms. The weighting scheme employed was $w = [\sigma^2(F_o^2) + (0.1377 \cdot P)^2 + (0.9991 \cdot P)]$, $P = (|F_o|^2 + 2|F_c|^2)/3$; and the goodness of fit on F^2 was 1.043 for all observed reflections. For **3**, convergence was reached at a final $R1 = 0.0375$ [for $I > 2\sigma(I)$], $wR2 = 0.1027$ [for all data], 114 parameters, with allowance for the thermal anisotropy for all non-hydrogen atoms. The weighting scheme employed was $w = [\sigma^2(F_o^2) + (0.0562 \cdot P)^2 + (1.2574 \cdot P)]$, $P = (|F_o|^2 + 2|F_c|^2)/3$; and the goodness of fit on F^2 was 1.065 for all observed reflections. Crystal data and details on the data collection and refinement are summarized in Table 5. CCDC-156272 for **1**, -156273 for **2**, and -156274 for **3** contain the supplementary crystallographic data for this paper. These data can be obtained free of charge at www.ccdc.cam.ac.uk/conts/retrieving.html or from the Cambridge Crystallographic Data Centre, 12 Union Road, Cambridge CB2 1EZ, UK [Fax: (internat.) + 44-1223/336-033; E-mail: deposit@ccdc.cam.ac.uk].

Acknowledgments

This research was supported by Dirección General de Investigación Científica y Técnica (Grant BQ2000/0791), G. F. received a PhD Grant from Universitat de Barcelona.

[1] S. V. Antonyuk, V. R. Melikadamyan, A. N. Popov, V. S. Lamzin, P. D. Hempstead, P. M. Harrison, P. J. Artymyuk, V. V. Barynin, *Crystallogr. Rep.* **2000**, *45*, 105−116.
[2] M. C. J. Wilce, C. S. Bond, N. E. Dixon, H. C. Freeman, J. M. Guss, P. E. Lilley, J. A. Wilce, *Proc. Nat. Acad. Sci. Usa* **1998**, *95*, 3472−3477.
[3] M. C. Bewley, P. D. Jeffrey, M. L. Patchett, Z. F. Kanyo, E. N. Baker, *Struct. Fold. Des.* **1999**, *7*, 435−448.
[4] G. B. Conyers, G. Wu, M. J. Bessman, A. S. Mildvan, *Biochemistry* **2000**, *39*, 2347−2354.
[5] S.-B. Yu, A. Bino, I. Shweky, S. J. Lippard, *Inorg. Chem.* **1992**, *31*, 3502−3504.
[6] A. Caneschi, F. Ferraro, D. Gatteschi, M. Ch. Melandri, P. Rey, R. Sessoli, *Angew. Chem. Int. Ed. Engl.* **1989**, *28*, 1365−1367.
[7] B. H. Ye, T. Mak, I. D. Williams, X. Y. Li, *Chem. Commun.* **1997**, 1813−1814.
[8] U. Bossek, K. Wieghardt, B. Nuber, J. Weiss, *Inorg. Chim. Acta* **1989**, *165*, 123−129.
[9] K. Wieghardt, U. Bossek, B. Nuber, J. Weiss, J. Bonvoisin, M. Corbella, S. E. Vitols, J.-J. Girerd, *J. Am. Chem. Soc.* **1988**, *110*, 7398−7411.
[10] M. Mikuriya, T. Fujii, T. Tokii, A. Kawamori, *Bull. Chem. Soc. Jpn.* **1993**, *66*, 1675−1686.
[11] Y. Gultneh, A. Farooq, S. Liu, K. D. Karlin, J. Zubieta, *Inorg. Chem.* **1992**, *31*, 3607−3611.
[12] H. Sakiyama, H. Tamaki, M. Kodera, N. Matsumoto, H. Okawa, *J. Chem. Soc., Dalton Trans.* **1993**, 591−595.
[13] C. Higuchi, H. Sakiyama, H. Okawa, R. Isobe, D. E. Fenton, *J. Chem. Soc., Dalton Trans.* **1994**, 1097−1103.
[14] C. Higuchi, H. Sakiyama, H. Okawa, D. E. Fenton, *J. Chem. Soc., Dalton Trans.* **1995**, 4015−4020.
[15] U. P. Singh, R. Singh, S. Hikichi, M. Akita, Y. Moro-oka, *Inorg. Chim. Acta* **2000**, *310*, 273−278.
[16] H. Matsushima, E. Ishiwa, M. Koikawa, M. Nakashima, T. Tokii, *Chem. Lett.* **1995**, 129−130.
[17] M. Yamami, M. Tanaka, H. Sakiyama, T. Koga, K. Kobaya-

shi, H. Miyasaka, M. Ohba, H. Okawa, *J. Chem. Soc., Dalton Trans.* **1997**, 4595−4601.
[18] M. Osawa, U. P. Singh, M. Tanaka, Y. Morooka, N. Kitajima, *J. Chem. Soc., Chem. Commun.* **1993**, 310−311.
[19] B. Albela, M. Corbella, J. Ribas, I. Castro, J. Sletten, H. Stoeckli-Evans, *Inorg. Chem.* **1998**, *37*, 788−798.
[20] R. L. Rardin, W. B. Tolman, S. J. Lippard, *New J. Chem.* **1991**, *15*, 417−430.
[21] C.-M. Che, W.-T. Tang, K.-T. Wong, W.-T. Wong, T.-F. Lai, *J. Chem. Research (S)* **1991**, 30.
[22] H. Oshio, E. Ino, I. Mogi, T. Ito, *Inorg. Chem.* **1993**, *32*, 5697−5703.
[23] B. Albela, M. Corbella, J. Ribas, *Polyhedron* **1996**, *15*, 91−96.
[24] T. Tanase, S. J. Lippard, *Inorg. Chem.* **1995**, *34*, 4682−4690.
[25] C. H. Kennard, G. Smith, E. O′Reilly, W. Chiangjin, *Inorg. Chim. Acta* **1983**, *69*, 53−59.
[26] T. Glowiak, H. Kozlowski, L. S. Erre, G. Micera, *Inorg. Chim. Acta* **1995**, *236*, 149−154.
[27] H. Iikura, T. Nagata, *Inorg. Chem.* **1998**, *37*, 4702−4711.
[28] M. McCann, M. T. Casey, M. Devereux, M. Curran, G. Ferguson, *Polyhedron* **1997**, *16*, 2547−2552.
[29] J. Kim, J. M. Lim, M. C. Suh, H. Yun, *Polyhedron* **2001**, *20*, 1947−1951.
[30] H. Adams, N. A. Bailey, N. Debaecker, D. E. Fenton, W. Kanda, J. M. Latour, H. Okawa, H. Sakiyama, *Angew. Chem. Int. Ed. Engl.* **1995**, *34*, 2535−2537.
[31] X.-M. Chen, Y.-X. Tong, Z.-T. Xu, T. C. W. Mak, *J. Chem. Soc., Dalton Trans.* **1995**, 4001−4004.
[32] S. Ménage, S. E. Vitols, P. Bergerat, E. Codjovi, O. Kahn, J.-J. Girerd, M. Guillot, X. Solans, T. Calvet, *Inorg. Chem.* **1991**, *30*, 2666−2671.
[33] R. L. Rardin, P. Poganiuch, A. Bino, D. P. Goldberg, W. B. Tolman, S. Liu, S. J. Lippard, *J. Am. Chem. Soc.* **1992**, *114*, 5240−5249.
[34] G. Christou, *Acc. Chem. Res.* **1989**, *22*, 328−335.
[35] V. Tangoulis, D. A. Malamatari, K. Soulti, V. Stergiou, C. P. Raptopoulou, A. Terzis, T. A. Kabanos, D. P. Kessissoglou, *Inorg. Chem.* **1996**, *35*, 4974−4983.
[36] R. L. Rardin, A. Bino, P. Poganiuch, W. B. Tolman, S. Liu, S. J. Lippard, *Angew. Chem. Int. Ed. Engl.* **1990**, *29*, 812−814.
[37] Z. J. Zhong, X. Z. You, *Polyhedron* **1994**, *13*, 2157−2161.
[38] M. J. Baldwin, J. W. Kampf, V. L. Pecoraro, *J. Chem. Soc., Chem. Commun.* **1993**, 1741−1743.
[39] Z. Sun, P. K. Gantzel, D. N. Hendrickson, *Polyhedron* **1998**, *17*, 1511−1516.
[40] M. J. Baldwin, J. W. Kampf, M. L. Kirk, V. L. Pecoraro, *Inorg. Chem.* **1995**, *34*, 5252−5260.
[41] E. Colacio, J. M. Dominguezvera, M. Ghazi, R. Kivekas, M. Klinga, J. M. Moreno, *Eur. J. Inorg. Chem.* **1999**, 441−445.
[42] C. Policar, F. Lambert, M. Cesario, I. Morgenstern-Badarau, *Eur. J. Inorg. Chem.* **1999**, 2201−2207.
[43] Z. Sun, P. K. Gantzel, D. N. Hendrickson, *Polyhedron* **1997**, *16*, 3267−3271.
[44] X. S. Tan, D. F. Xiang, W. X. Tang, K. B. Yu, *Polyhedron* **1997**, *16*, 1411−1415.
[45] M. Devereux, M. Curran, M. McCann, M. T. Casey, V. McKee, *Polyhedron* **1996**, *15*, 2029−2033.
[46] J. Cano, G. Demunno, J. Sanz, R. Ruiz, F. Lloret, J. Faus, M. Julve, *J. Chem. Soc., Dalton Trans.* **1994**, 3465−3469.
[47] X. S. Tan, J. Sun, D. F. Xiang, W. X. Tang, *Inorg. Chim. Acta* **1997**, *255*, 157−161.
[48] M. E. Fisher, *Am. J. Phys.* **1964**, *32*, 343.
[49] T. L. Stemmler, T. M. Sossong, Jr., J. I. Goldstein, D. E. Ash, T. E. Elgren, D. M. Kurtz Jr, J. E. Penner-Hahn, *Biochemistry* **1997**, *36*, 9847−9858.
[50] The simulation software package is freely distributed by Dr. H. Weihe; for more information see the www page: http://sophus.kiku.dk/software/epr/epr.html
[51] G. M. Sheldrick, *SADABS, Program for absorption corrections using Bruker CCD data*, University of Göttingen, Germany, **1996**.
[52] G. M. Sheldrick, *Bruker SHELXTL-PC*, University of Göttingen, Germany, **1997**.

Received April 16, 2002
[I02198]